DOI 10.1007/s10812-016-0306-1
Journal of Applied Spectroscopy, Vol. 83, No. 3, July, 2016 (Russian Original Vol. 83, No. 3, May–June, 2016)

DETERMINATION OF THE CHARACTERISTICS OF GROUND-BASED IR SPECTRAL INSTRUMENTATION FOR ENVIRONMENTAL MONITORING OF THE ATMOSPHERE

M. V. Makarova,[a*] A. V. Poberovskii,[a] F. Hase,[b] Yu. M. Timofeyev,[a] and Kh. Kh. Imhasin[a]

UDC543.42.062:551.51

This is a study of the spectral characteristics of a ground-based spectral system consisting of an original system for tracking the sun developed at St. Petersburg State University and a Bruker IFS125HR Fourier spectrometer. The importance of accounting for the actual instrument function of the spectral system during processing of ground-based IR spectra of direct solar radiation is illustrated by the example of determining the overall abundance of methane in the atmosphere. Spectral intervals are proposed for taking spectra of direct solar radiation with an HBr cell, which yield information on the parameters of the ground-based system, while simultaneously checking the alignment of the system for each spectrum of the atmosphere.

Keywords: *atmospheric IR Fourier spectrometry, gas composition of the atmosphere, IR spectra of direct solar radiation, transmission spectra of HBr cells, instrument function of Fourier spectrometer.*

Introduction. IR spectroscopic techniques are widely used for research in various areas of chemistry and physics [1]. Fourier spectrometers with medium and high spectral resolution are used in experimental studies of the gaseous composition of the atmosphere employing ground-based [2, 3], satellite [4–6], and airborne [7] measurement systems. The most important minor gaseous components of the atmosphere from the standpoint of climate and chemical activity (H_2O, CO_2, CH_4, N_2O, CO, O_3, etc.) have absorption bands in the IR, so that transmission spectra can be used to obtain information on the composition of the atmosphere. An international network for observing changes in the gaseous composition of the atmosphere (NDACC, Network for the Detection of Atmospheric Composition change) [8] has been in existence for more than twenty years. The stations in this network, which are part of the IRWG (Infrared Working Group) [2] are equipped with high resolution Fourier spectrometers. In 2004 measurements were begun at the TCCON (Total Carbon Column Observing Network) Fourier monitoring stations [3]. Similar measurements have been made in Russia since 2009 at two stations: the atmospheric monitoring station "Peterhof" (St. Petersburg State University) [2, 9–13] and the atmospheric Fourier station of the Urals Federal University (UrFU) [14, 15].

Modern Fourier spectrometers can record solar radiation spectra over a wide range with a high signal/noise ratio. The spectral resolution of the Bruker IFS125HR Fourier spectrometers (~0.002 cm^{-1}) used in atmospheric measurements is high enough to resolve profiles of individual spectrum lines. Given the pressure dependence of a line profile, this in turn means that information can be obtained on the overall amount of a gas over the entire thickness of the atmosphere, but also on the vertical distribution of some gas components [13, 16–18]. Monitoring data on the atmosphere from the NDACC and TCCON stations are used in campaigns to validate satellite measurements of the gas composition, in studies of temporal variations in the amounts of minor gas constituents of the atmosphere, and in comparisons with computer models [12, 15, 19–22]. The demands for accuracy in measurements of the quantitative characteristics of the gas composition are high, so strict monitoring of the state of the measuring instruments and knowledge of their characteristics are needed for correct determination of the overall amount or distribution of a gas in the atmosphere [23]. For this purpose, regular measurements of the transmission spectra of cells filled with a gas with a high molecular weight at low pressure are made in the NDACC and TCCON networks [24–26].

*To whom correspondence should be addressed.

[a]St. Petersburg State University, 3 Ul′yanovskaya Str., St. Petersburg, 198504, Russia; [b]Institute of Meteorology and Climate Research, Karlsruhe Institute of Technology, Karlsruhe, Germany; e-mail: zaits@troll.phys.spbu.ru. Original article submitted January 15, 2016. Translated from Zhurnal Prikladnoi Spektroskopii, Vol. 83, No. 3, pp. 437–444, May–June, 2016.

These measurements are processed with the specialized LINEFIT program [27] to determine the instrument function, which provides information on the quality of alignment of the Fourier spectrometer.

This paper is a study of the characteristics of a ground-based spectral system consisting of an original system for tracking the sun developed at St. Petersburg State University [28] and a Bruker IFS125HR Fourier spectrometer. The results are based on analyzing transmission spectra of an HBr cell illuminated by an internal source in the Fourier spectrometer as well as by the sun. In the first case (internal illuminator) the spectra of the HBr cell only contain information on the quality of alignment of the interferometer itself, and in the second (solar measurements), on the quality of alignment of the optics of the spectral system as a whole, including the external solar tracking system as well as the interferometer. The standard spectral intervals used by LINEFIT for processing the spectra of the HBr cell obtained with the internal source in the Fourier spectrometer cannot be used for the solar measurements because of interfering absorption lines of atmospheric gases. We propose spectral intervals that can provide information on the instrument function (alignment quality) of a ground-based spectral system for every atmospheric spectrum that is recorded jointly with an HBr cell.

Measurement Technique and Data Analysis. The following factors were taken into account when choosing the fill gas for the cell (which is used subsequently to determine the quality of the alignment of the Fourier spectrometer): the spectrum lines of the gas must be narrower than or comparable to the resolution of the Fourier spectrometer (usually ~0.005–0.008 cm^{-1}); isolated lines of the gas which do not overlap lines of the atmospheric gases are desirable in the IR; small concentrations or complete absence of the gas in atmospheric air; and, slow variation (owing to chemical reactions) in the concentration of the gas in the cell over time. The cells are most often filled with the following gases HBr, N_2O, C_2H_6, and HCl (where HCl and HBr are less stable) [24–26].

In our experiments we used cell #61 which was fabricated for the NDACC network. It has a length of 2 cm, sapphire wedge windows, and is filled with HBr to a low pressure (~2.3 mbar). In this case, Doppler broadening determines the spectral line profiles of HBr and for a wave number of ~2500 cm^{-1} and T = 294 K the half width of the HBr line is ~0.0034 cm^{-1}. Transmission spectra in the absorption band of HBr (isotopes HBr^{79} and HBr^{81}) centered at ~2559 cm^{-1} are usually measured at least twice a year. The transmission spectra are processed by the LINEFITv.14 program, which is based on fitting a calculated spectrum to the measured spectrum using regularization algorithms employed for solving incorrectly stated inverse problems in atmospheric optics [27]. The HITRAN2008 spectroscopic data base [29] is used in analyzing the spectra. The LINEFIT results are in good agreement with the results of other algorithms for determining the parameters of Fourier spectrometers [25, 30].

The most important input data for LINEFIT are the transmission spectrum of the cell, the optical path difference (of light in the interferometer), and the apodization functions used during recording of the spectrum, as well as the temperature and pressure of the gas in the cell. The main output parameters are the instrument function (IF) of the Fourier spectrometer, the modulation efficiency (ME), the phase error (PE), and the gas content in the cell. In addition it is also possible to determine the temperature and pressure of the gas in the cell. Here the modulation efficiency is taken to be ratio of the normalized amplitudes of the modulation of the actual Fourier spectrometer and the modulation of an "ideal" Fourier spectrometer as a function of the optical path difference. The term "normalized" means that the modulation amplitude for zero optical path difference equals 1. (This is necessary in order to preserve the necessary normalization with respect to area for the instrument function [24, 25].) We note that in the model of an "ideal" Fourier spectrometer (set in the LINEFIT program) only the finiteness of the optical path difference and the presence of a self-apodization effect have been taken into account [24]. Modulation losses, which are characterized in our case by the modulation efficiency function, lead to broadening of the instrument function, while the presence of phase error (rapid changes in the phase error function) leads to asymmetry in the instrument function [25]. It should be noted that the Bruker IFS125HR Fourier spectrometer is highly stable and we are concerned here only with small misalignments of its optical system.

Processing of the cell spectra yields the IF, ME, and PE functions and provides monitoring of the amount of HBr in the cell (w_{HBr}). This is necessary, first, as a supplementary estimate of the quality of the analysis of the spectra (no sharp changes in w_{HBr} should be observed from one measurement to the next; typically the variation in the content is ≤1%) and, second, as a way of tracking the rate of decomposition of the HBr in the cell. Here it is desirable to have a "standard" value of w_{HBr} determined with high accuracy in independent measurements (this is usually done immediately after the cell is filled with gas). For this, the transmission spectra of two cells are measured simultaneously on a similar apparatus (Bruker IFS125HR Fourier spectrometer) at the Karlsruhe Institute of Technology (KIT): cell HBr #61 and an N_2O cell (length 0.4 m) with a known pressure (1.004 mbar). During processing of the spectrum, the IF (ME and PE) of the KIT Fourier Spectrometer are first measured using absorption lines of N_2O in the interval 2529.4–2550.5 cm^{-1}. Then the known IF (N_2O) is used to

TABLE 1. Spectral Intervals for Determining the Instrument Function, Modulation Efficiency Function, and Phase Error Function Based on Laboratory Transmission Spectra of Hbr Cells and on Solar Spectra

HBr *R*-branch microwindow, cm^{-1}	HBr *P*-branch microwindow, cm^{-1}	HBr *P*-branch microwindow (sun), cm^{-1}
2590.32–2590.72	2412.48–2412.88	2412.58–2412.88
2590.71–2591.11	2412.80–2413.20	2412.80–2413.10
2605.60–2606.00	2432.20–2432.60	2432.25–2432.46
2606.00–2606.40	2432.53–2432.93	2432.63–2432.83
2620.39–2620.79	2451.49–2451.89	2451.59–2451.75
2620.80–2621.20	2451.95–2452.15	2451.95–2452.15
2634.70–2635.10	2470.38–2470.78	2470.48–2470.68
2635.10–2635.50	2470.74–2471.14	2470.84–2471.00
2648.50–2648.90	2488.85–2489.25	–
2648.90–2649.30	2489.21–2489.61	2489.36–2489.51
2661.76–2662.16	2506.90–2507.30	2507.02–2507.20
2662.18–2662.58	2507.25–2507.65	–
2674.52–2674.92	2524.48–2524.88	2524.62–2524.78
2674.94–2675.34	2524.95–2525.15	2524.95–2525.15

determine the amount of HBr in that cell based on absorption lines of HBr (separately in the *P*- and *R*-branches of the bands). Fourteen microwindows containing absorption lines of HBr (see Table 1) are used for each of the absorption branches of HBr. These sets of microwindows are used to determine the IF, ME, and PE functions based on all the cell measurements made with the internal artificial light source of the Fourier spectrometer.

The R-branch microwindows of HBr were not used for the solar spectra (when the atmospheric transmission and the cell transmission are measured simultaneously). This is because, as opposed to the *P*-branch, the lines in the *R*-branch overlap more strongly with interfering lines of atmospheric gases. Since the LINEFIT procedure for processing the spectra does not include an algorithm to account for absorption by the entire thickness of the atmosphere, the presence of lines of the atmospheric gases makes it impossible to determine the IF, ME, and PE functions correctly. For this reason the set of lines in and the widths of the *P*-branch microwindows are modified so as to exclude the central parts of atmospheric absorption lines from the microwindows. The effect of the wings of atmospheric lines is taken into account by the choice of polynomial approximation. The modified set of 12 microwindows proposed for processing simultaneous measurements of the atmosphere and a cell is listed in the last column of Table 1. An example of measured (February 2, 2015, solar) and calculated spectra in the 2470.48–2470.68 cm^{-1} microwindow, together with the difference between them, is shown in Fig. 1. Also shown there are the positions of interfering atmospheric N_2O lines that are observed in the wider standard interval 2470.38–2470.78 cm^{-1} used for processing laboratory spectra of the cell with HBr.

Results and Discussion. Table 2 lists the main characteristics of the laboratory and solar spectra of the HBr cell in chronological order, along with the values of w_{HBr} obtained after processing these spectra with the LINEFIT program (for measurements with the internal light source for the *P*- and *R*-branches). It can be seen that for all the spectra taken with the internal source the amounts of HBr in the cell found by processing the microwindows in the *R*-branch are an average of ~1.5% higher than the analogous values for the *P*-branch. The most probable reason for this is systematic errors in the spectroscopic data for HBr in the HITRAN2008 data base. Thus, for long-term analysis of the behavior of the IF, ME, and PE functions and the HBr content in the cell, it is best to use measurements within a given branch of the HBr band. In our case the optimum is the *P*-branch of the HBr absorption band since, as noted above, this branch can be analyzed for the solar spectra. Against the background of fluctuations in w_{HBr} from measurement to measurement, the rate of decrease in w_{HBr} associated with chemical decomposition of HBr in the cell was ~0.4 %/year during 2012–2015 (Table 2).

Figures 2 and 3 show the IF, ME, and PE functions for the Bruker IFS125HR Fourier spectrometer at St. Petersburg State University for transmission spectra of the HBr cell taken with the internal source during 2012–2014. The differences in the instrument functions of the Fourier spectrometer for different dates are small, and the IF curves essentially coincide in Fig. 3 (for this reason, the more intuitive ME and PE functions are more often used).

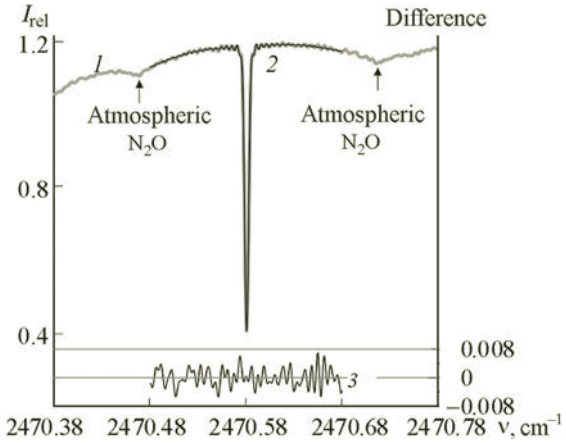

Fig. 1. Measured (on February 17, 2015) spectrum of the sun (1) and a calculated spectrum (2) in the 2470.48–2470.68 cm^{-1} microwindow, together with the difference between them (3).

TABLE 2. Major Characteristics of Laboratory (L) and Solar (S) Spectra Measured with an HBr Cell, Including the HBr Content Found from the *P*- and *R*-Branches of the Absorption Band of HBr

Observation date (site*)	Type of spectrum**	Aperture, mm	Number of scans	*S/N*	w_{HBr_P}, 10^{21} m^{-2}	w_{HBr_R}, 10^{21} m^{-2}
10.04.2012	L	1.15	25	~900	1.123 ± 0.003	1.130 ± 0.003
09.07.2012	L	1.15	100	~1700	1.123 ± 0.003	1.138 ± 0.001
20.05.2013	L	1.15	100	~1400	1.128 ± 0.003	1.158 ± 0.003
02.05.2014 (KIT)	L	0.8	20	~2000	1.112 ± 0.005	1.134 ± 0.001
03.10.2014	L	1.15	50	~1000	1.113 ± 0.003	1.118 ± 0.003
Series (16–17).02.2015	S, *SZA* = 72–73°	1.15	10–30	~500	1.107 ± 0.005	–
17.02.2015	L	1.15	50	~1700	1.105 ± 0.003	1.120 ± 0.002
04.09.2015	L	1.15	100	~1900	1.110 ± 0.002	1.125 ± 0.001
Series 11.09.2015	S, *SZA* = 56–57°	1.15	10	~500	1.113 ± 0.002	–

*Observation site is St. Petersburg State University unless otherwise indicated.

**For all the measurements the optical path difference is 180 cm (for the Bruker IFS125HR Fourier spectrometer this corresponds to a spectral resolution of 0.005 cm^{-1}); the apodization function is the boxcar.

When processing the solar spectra (HBr cell and atmosphere) the changes in the atmospheric transmission (this effect is always present owing to changes in the sun's position and the instability of the atmosphere itself) during recording of the interferograms is interpreted as variations in the ME, which leads to corresponding changes in the IF. The optical path lengths from the internal source and from the sun are the same inside the interferometer (as part of the IF), but the flux of solar radiation is directed into the interferometer by the solar tracking system, the operating quality of which does influence the IF, ME, and PE functions. Although the intervals for processing the solar spectra were chosen so as to exclude the centers of atmospheric absorption lines, it was not possible to eliminate the influence of atmospheric lines entirely. They can cause jumps in the PE function that are unrelated to the actual operation of the tracking system and the interferometer; i.e., increased errors in determining the ME and PE that have been estimated [25] at ~1–2%. These factors together can lead to differences in the IF, ME, and PE functions obtained only for the Fourier spectrometer (measured with the internal source) and for the spectral system as a whole (solar measurements) [25].

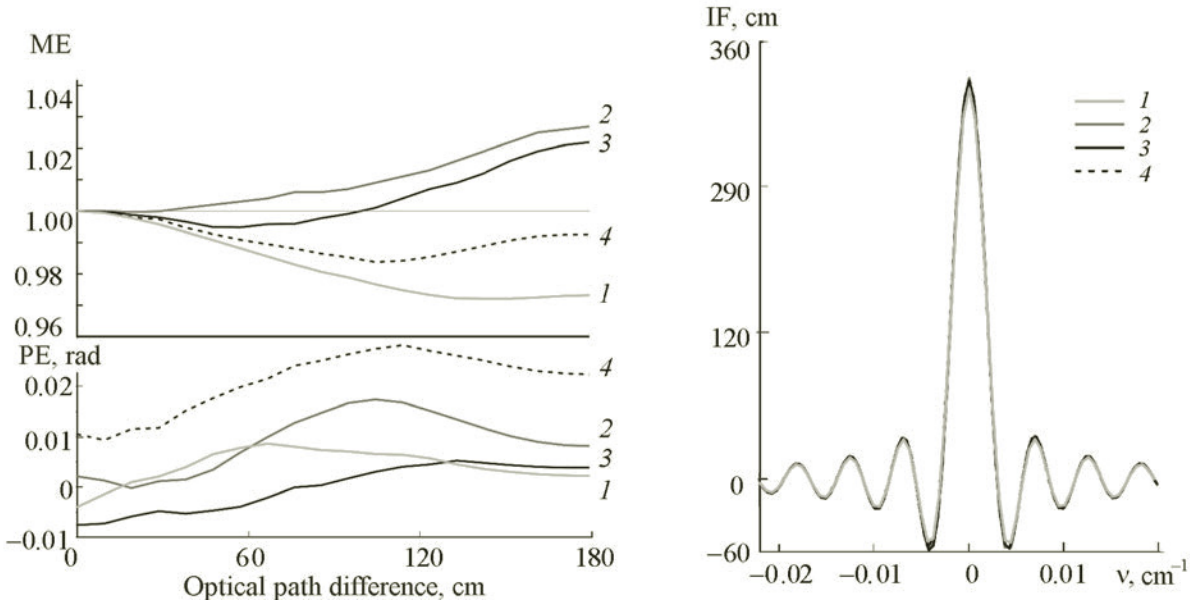

Fig. 2. The ME and PE functions for the Bruker IFS125HR Fourier spectrometer (at St. Petersburg State University) derived from measurements of the transmission spectrum of an HBr cell with the internal light source on April 10, 2012 (1), July 9, 2012 (2), May 20, 2013 (3), and October 3, 2014 (4).

Fig. 3. Instrument functions of the Bruker IFS125HR Fourier spectrometer (at St. Petersburg State University) derived from measurements of laboratory transmission spectra of HBr on April 10, 2012 (1), July 9, 2012 (2), May 20, 2013 (3), and October 3, 2014 (4).

Measurements of the ME and PE functions derived from spectra of the internal source in the Fourier spectrometer and of the sun in two series of measurements during February and September 2015 are compared in Fig. 4. In the first case, the measurements were made over two successive days (February 16 and 17) and in the second, a week apart (September 4 and 11). The solar zenith angles (SZA) at which the atmospheric measurements were made together with the HBr cell are given in Table 2 (column 2). Usually a single solar spectrum is taken in ~12 min (10 interferograms), but in the February series one spectrum (February 17) was obtained from 30 interferograms (~37 min). It is clear that the agreement between the ME functions for the laboratory and solar measurements is better in the February series. Such agreement was not obtained in September, possibly because the measurements with the sun and the internal source were made a week apart, but also because of the operation of the solar tracking system. It should be noted that difference between the values of the ME function based on the solar and laboratory spectra in the September measurements is also small (<2%).

All the PE functions in Fig. 4 are similar in shape, but for the solar measurements they are systematically higher than the functions derived from the laboratory measurements. The main reasons for these differences in the PE functions are the effect of the atmosphere and the presence of additional optical components (optical filters used to isolate the required spectral intervals for the direct solar measurements; the solar tracking system) that are usually absent in the laboratory measurements with the internal source. Our experiments showed that in laboratory measurements of the HBr cell with and without the optical filters used in the solar measurements, systematic shifts of the PE functions relative to one another could be seen while the shape of the functions was retained. The results of the IF determination are not shown since even in the September series the instrument functions derived from the laboratory and solar measurements were essentially indistinguishable.

The main value of simultaneous measurements of the cell and atmosphere is the possibility of determining the IF, ME, and PE functions for a specific solar spectrum recorded by the spectral system. Use of these functions for subsequent processing of the atmospheric part of the spectrum makes it possible to achieve greater accuracy in determining the overall content and profiles of atmospheric gases. We illustrate this for atmospheric methane in three solar spectra

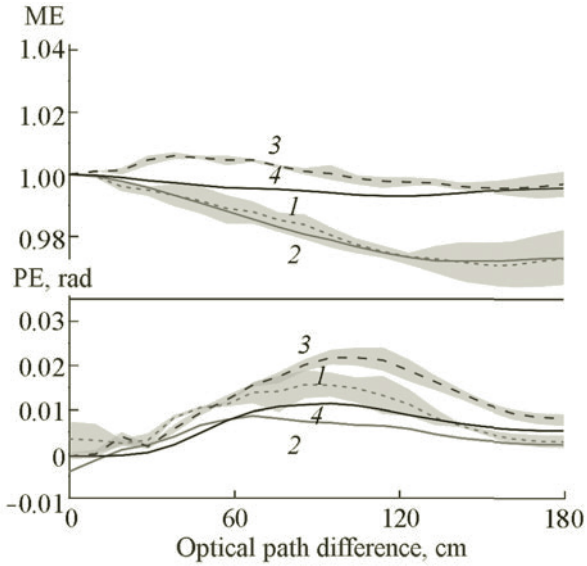

Fig. 4. The ME and PE functions derived from spectra of the internal illuminator of the Fourier spectrometer (2, 4) and the sun (1, 3) during February (1, 2) and September (3, 4) 2015; the gray region surrounding the dashed curves is the range of variation of the ME and PE functions for the solar measurements.

TABLE 3. Results of Processing Solar Spectra with Different Forms of Instrument Function

Date, time	OC_i CH_4, 10^{19} cm^{-2} (RMS, %)	OC_r CH_4, 10^{19} cm^{-2} (RMS, %)	Relative difference between OC_r and OC_i, %
11.09.2015, 13:32	3.992 (0.22)	4.048 (0.20)	1.4
11.09.2015, 13:45	3.989 (0.22)	4.044 (0.20)	1.4
11.09.2015, 13:57	4.002 (0.22)	4.053 (0.20)	1.3

(atmosphere together with the HBr cell) from the September 11, 2015, series. Table 3 lists the overall content (OC) of methane over the entire thickness of the atmosphere obtained by processing these spectra with different instrument functions: OC_i with the IF of an "ideal" Fourier spectrometer (i.e., the ME and PE functions are equal to 1 and 0 over the entire range of optical path differences), OC_r with an IF that includes the real features of the IF of the spectral system (the ME and PE functions derived from the sun for September 11, 2015 and shown as the dashed curves in Fig. 4). Table 3 also lists the mean square difference between the measured and calculated spectra (RMS, %) in the standard microwindows 2613.7–2615.4, 2835.5–2835.8, and 2921.0–2921.6 cm^{-1} [23], used in the NDACC network for determining the overall content of CH_4 in the atmosphere. It is clear that the quality of the fit of the calculated spectrum to the measured spectrum (which is the objective criterion for the quality of the solution of the inverse atmospheric optics problem) is best for the real IF of the spectral system. Here the average difference between the overall content in the second and third columns is ~1.3%, which is higher than current specifications for the accuracy in determining the overall content of atmospheric CH_4 (~0.3%) [23].

Conclusions. Spectral intervals have been proposed for use in simultaneous measurements of the transmission spectra of the atmosphere and of an HBr cell (with the sun as the light source) for determining the instrument function, modulation efficiency, and phase error of a high-resolution spectral system. The results derived from laboratory and solar spectra of an HBr cell yielded good (±2%) agreement of the modulation efficiency functions. The phase shifts for the solar and laboratory spectra differed systematically owing to the influence of interfering lines of atmospheric gases, as well as the presence of additional optical components in the spectral system (optical filters and a solar tracking system)

for use in solar measurements. An analysis of solar spectra for a series of September 11, 2015, in which simultaneous measurements of the atmosphere and an HBr cell were made, shows that when the instrument functions of an ideal Fourier spectrometer and of the real spectral system were used, the difference in the overall content of CH_4 over the entire depth of the atmosphere can be >1%. An analysis of the transmission spectrum of the HBr cell showed that the loss of modulation amplitude was ≤5% for the Bruker IFS125HR Fourier spectrometer at St. Petersburg State University during 2012–2015. Variations in the phase errors, which can lead to significant asymmetry of the instrument function of the Fourier spectrometer, were not observed. This indicates that the alignment of the Fourier interferometer was satisfactory during 2012–2015. The estimated rate of loss of HBr in the cell (#61 NDACC) owing to decomposition of HBr was ~0.4%/year during the 2012–2015 period.

These experiments were partially supported by a grant from St. Petersburg State University (11.42.1430.2015, Program 6). The Data were processed and analyzed with support from the Russian Science Foundation (No. 14-17-00096). The measurements were made using equipment of the “Geomodel" resource center at St. Petersburg State University.

REFERENCES

1. P. R. Grifiths and J. A. de Haseth, *Fourier Transform Infrared Spectrometry*, John Wiley & Sons, Inc., Hoboken, New Jersey (2007), pp. 1–3.
2. Observational network IRWG/NDACC: https://www2.acom.ucar.edu/irwg
3. Observational network TCCON: https://tccon-wiki.caltech.edu/
4. Satellite experiment GOSAT: http://www.gosat.nies.go.jp/en/
5. Satellite experiment IASI: http://www.eumetsat.int/website/home/Satellites/CurrentSatellites/Metop/MetopDesign/IASI/index.html
6. Spacecraft Meteor-M No. 2: http://planet.iitp.ru/index1.html
7. Remote sensing using aircraft and balloons: https://www.imk-asf.kit.edu/english/ffb.php
8. Observational network NDACC: http://www.ndsc.ncep.noaa.gov/
9. RTs Geomodel: http://geomodel.spbu.ru/
10. M. V. Makarova, O. Kirner, Yu. M. Timofeev, A. V. Poberovskii, Kh. Kh. Imkhasin, V. I. Osipov, and B. K. Makarov, *Izv. Ross. Akad. Nauk*, *Fiz. Atm. Okeana*, **51** (2), 201–209 (2015).
11. Ya. A. Virolainen, Yu. M. Timofeev, A. V. Poberovskii, M. Eremenko, and G. Dufor, *Izv. Ross. Akad. Nauk*, *Fiz. Atm. Okeana*, **51** (2), 191–200 (2015).
12. A. V. Polyakov, Yu. M. Timofeev, A. V. Poberovskii, and Ya. A. Virolainen, *Opt. Atm. Okeana*, **28** (2), 153–158 (2015).
13. M. V. Makarova, O. Kirner, Yu. M. Timofeev, A. V. Poberovskii, Kh. Kh. Imkhasin, V. I. Osipov, and B. K. Makarov, *Izv. Ross. Akad. Nauk*, *Fiz. Atm. Okeana*, **51** (2), 493–501 (2015).
14. UrFU atmospheric Fourier station: http://wsibiso.ru/index.php?option=com_content&view=article&id=68&Itemid=60&lang=ru
15. N. V. Rokotyan, R. Imasu, V. I. Zakharov, K. G. Gribanov, and M. Yu. Khamatnurova, *Opt. Atm. Okeana*, **27** (9), 819–825 (2014).
16. E. Sepúlveda, M. Schneider, F. Hase, O. E. García, A. Gomez-Pelaez, S. Dohe, T. Blumenstock, and J. C. Guerra, *Atm. Meas. Tech*., **5**, 1425–1441 (2012).
17. O. E. García, M. Schneider, A. Redondas, Y. González, F. Hase, T. Blumenstock, and E. Sepúlveda, *Atm. Meas. Tech*., **5**, 2917–2931 (2012).
18. M. Schneider, E. Sepúlveda, O. García, F. Hase, and T. Blumenstock, *Atm. Meas. Tech*., **3**, 1785–1795 (2010).
19. N. M. Gavrilov, M. V. Makarova, A. V. Poberovskii, and Yu. M. Timofeyev, *Atm. Meas. Tech*., **7**, 1003–1010 (2014).
20. T. Kerzenmacher, B. Dils, N. Kumps, T. Blumenstock, C. Clerbaux, P.-F. Coheur, P. Demoulin, O. García, M. George, D. W. T. Griffith, F. Hase, J. Hadji-Lazaro, D. Hurtmans, N. Jones, E. Mahieu, J. Notholt, C. Paton-Walsh, U. Raffalski, T. Ridder, M. Schneider, C. Servais, and M. De Mazière, *Atm. Meas. Tech*., **5**, 2751–2761 (2012).
21. S. Takele Kenea, G. Mengistu Tsidu, T. Blumenstock, F. Hase, T. von Clarmann, and G. P. Stiller, *Atm. Meas. Tech*., **6**, 495–509 (2013).
22. Ya. Virolainen, Yu. Timofeyev, A. Polyakov, D. Ionov, and A. Poberovsky, *Int. J. Remote Sens.*, **35** (15), 5677–5697 (2014).

23. R. Sussmann, F. Forster, M. Rettinger, N. Jones, *Atm. Meas. Tech*., **4**, 1943–1964 (2011).
24. F. Hase, *Atm. Meas. Tech*., **5**, 603–610 (2012).
25. F. Hase, T. Blumenstock, and C. Paton-Walsh, *Appl. Opt*., **38**, 3417–3422 (1999).
26. A. Goldman, M. T. Coffey, J. W. Hannigan, W. G. Mankin, K. V. Chance, and C. P. Rinsland, *JQSRT*, **82**, 313–317 (2003).
27. Program LINEFIT: https://www.imk-asf.kit.edu/downloads/bod/linefit.pdf
28. A. V. Poberovskii, *Opt. Atm. Okeana*, **23** (1), 56–58 (2010).
29. L. S. Rothman, I. E. Gordon, A. Barbe, D. Chris Benner, P. F. Bernath, M. Birk, V. Boudon, L. R. Brown, A. Campargue, J.-P. Champion, K. Chance, L. H. Coudert, V. Dana, V. M. Devi, S. Fally, J.-M. Flaud, R. R. Gamache, A. Goldman, D. Jacquemart, I. Kleiner, N. Lacome, W. J. Lafferty, J.-Y. Mandin, S. T. Massie, S. N. Mikhailenko, C. E. Miller, N. Moazzen-Ahmadi, O. V. Naumenko, A. V. Nikitin, J. Orphal, V. I. Perevalov, A. Perrin, A. Predoi-Cross, C. P. Rinsland, M. Rotger, M. Simeckova, M. A. H. Smith, K. Sung, S. A. Tashkun, J. Tennyson, R. A. Toth, A. C. Vandaele, and J. Vander Auwera, *JQSRT*, **110**, 533–572 (2009).
30. C. Bernardo and D. W. T. Griffith, *JQSRT*, **95**, 141–150 (2005).